

Undercoordinated Ti Atoms as Oxygen Pumps on SrTiO₃(110) Surface

Fengmiao Li¹, Zhiming Wang¹, Yongbao Sun², Jinlong Yang², Sheng Meng¹, Qinlin Guo¹, and Jiandong Guo^{1*}

¹*Beijing National Laboratory for Condensed-Matter Physics & Institute of Physics,
Chinese Academy of Sciences, Beijing 100190, China and*

²*Hefei National Laboratory for Physical Science at the Microscale &
University of Science and Technology of China, Hefei, Anhui 230026, China*

(Dated: December 16, 2018)

The surface reconstruction of SrTiO₃(110) is studied with scanning tunneling microscopy and density functional theory (DFT) calculations. The reversible phase transition between (4×1) and (5×1) is induced by adjusting the surface metal concentration [Sr] or [Ti]. Resolving the atomic structures of the surface, DFT calculations verify that the phase stability changes upon the chemical potential of Sr or Ti. Particularly, the surface Ti atoms can draw O atoms from the bulk, forming fourfold coordinations to reach thermodynamic equilibrium.

PACS numbers: 68.47.Gh, 31.15.A-, 68.37.Ef, 68.35.Fx

Perovskite oxides have attracted intensive interests in the fields of fundamental condensed matter physics, photocatalysis chemistry, material science, as well as electronic applications, due to their rich phase diagrams and remarkable functionalities. The related research becomes even more exciting since the recent discovery of a quasi-two-dimensional electron gas (2DEG) between two insulating materials, SrTiO₃ and LaAlO₃ [1]. Subsequently, a tremendous amount of evidence has shown that the perovskite oxides in the low-dimensional (LD) form such as interfaces, thin films, or heterostructures display an equally rich diversity of exotic phenomena that is related, but not identical to the bulk [2–5], indicating a great opportunity for novel oxide-based devices [6, 7]. One of the most important and intriguing discoveries is that the atomic arrangement on the surface or at the interface is determinant for the properties of the entire artificial structure. Hwang *et al.* found that the formation of 2DEG critically depends on the type of atomic termination layer at the interface [1]. O vacancies also sensitively influence the density and mobility of the charge carriers at the heterointerface of LaAlO₃ and SrTiO₃ [8]. Therefore, to clarify the origin of the emergent properties in LD oxides and ultimately to tune them for the fabrication of functionalized devices, the detailed knowledge on their microscopic structures and the high-precision growth technique are the key issues.

Single crystalline SrTiO₃ is widely used as the epitaxial substrate for perovskite oxide films. In order to improve the growth quality, much effort has been made to obtain the atomically flat and ordered SrO or TiO₂ terminated (100) surface [9, 10]. In contrast to the electrically neutral (100) surface, the formation process of SrTiO₃(110) surface structure is much more complicated since it is inherently unstable due to the perpendicular macroscopic dipole formed by alternatively stacked (SrTiO)⁴⁺ and (O₂)⁴⁻ layers [11]. The (110) surface stoichiometry often deviates from that in the ideal crystal, which leads

to the formation of mixed phases of reconstruction [12]. Oxygen vacancies may also be responsible for the stabilization of the (110) surface [13]. Recently Russell *et al.* obtained an (*n*×1) (*n*=3,4,6) family of reconstructions at varying annealing temperatures, which was described as a homologous series with the TiO₄ tetrahedra model [14, 15]. However, it is still challenging to understand the stabilization mechanism of SrTiO₃(110) polar surface, particularly the behavior of oxygen (or vacancies) in the thermodynamic equilibrium picture.

In this letter, we investigate the microscopic structure of SrTiO₃(110) surface and present a way of preparing high-quality titanate surfaces and films with ideal oxygen stoichiometry. We obtain the monophased surface in (4×1) or (5×1) reconstruction. The reversible phase transition between them is realized by tuning Ti or Sr concentration on the surface. With *ab initio* calculations, we determine the atomic structures of both phases and study their thermodynamic stability in different chemical environments. Most importantly, we find that when the surface Ti atoms are undercoordinated they “pump” oxygen from the bulk that acts as an O reservoir. Such an “oxygen-pumping” mechanism suggests that the titanate (110) surface could be free of oxygen vacancy.

The experiments were performed in an Omicron ultra-high vacuum (UHV) low temperature scanning tunneling microscopy (STM) system with the base pressure of 1×10⁻¹⁰ mbar. Nb-doped (0.7 wt%) SrTiO₃(110) single crystals (12×3 mm²) were purchased from Hefei KMT Co., China. The as-received sample was sputtered with Ar⁺ beam at room temperature followed by annealing in UHV. Strontium and titanium were evaporated from Knudsen cells, respectively. The flux of Sr was calibrated by observing the formation of Sr/Si(001)-(2×1) reconstruction [16] with RHEED and STM, while the flux of Ti was calibrated by monitoring the RHEED intensity oscillation during the homoepitaxial growth

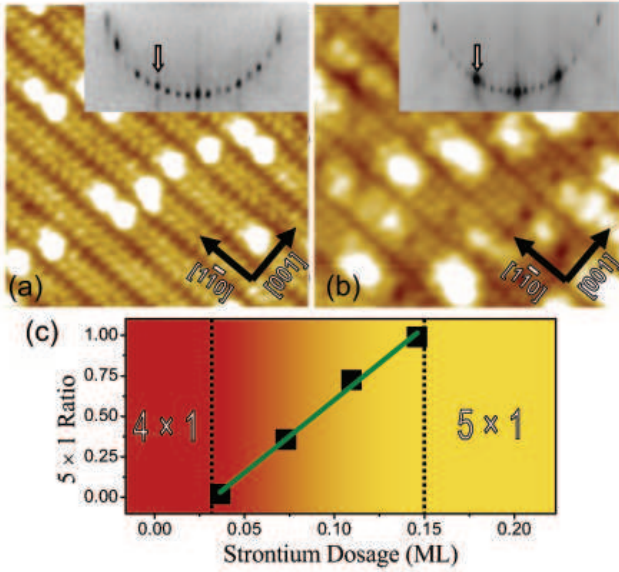


FIG. 1: (color online) (a) and (b) STM images ($15 \times 15 \text{ nm}^2$, 1.5 V/20 pA) of (4×1) and (5×1) reconstructed $\text{SrTiO}_3(110)$ surfaces, respectively. The insets show the RHEED patterns along $[001]$ direction with (10) spots indicated by arrows, respectively. (c) The area ratio of (5×1) domains through the entire surface depending on the Sr dosage. The statistics are done over 8 STM images ($500 \times 500 \text{ nm}^2$) for each data point.

of $\text{SrTiO}_3(110)$ film [17]. The sample was resistively heated by passing a direct current and the temperature was monitored with an infrared pyrometer. DFT calculations were carried out with the “Vienna *ab initio* simulation package” (VASP) code [18]. We use the projector augmented-wave (PAW) method [19] and the Perdew-Burke-Ernzerhof functional [20] with the kinetic energy cutoff of 400 eV for plane waves and a $(3 \times 5 \times 1)$ Monkhorst-Pack k -point mesh. The surface structure was modeled with a supercell that was symmetrical along the $[110]$ direction, consisted with a 13-layer slab separated by a vacuum layer of 12 Å. Atoms in the central three layers were fixed and other atoms were allowed to relax until the force on each atom was less than 0.02 eV/Å. Simulated STM images were generated by integrating the local density of states (LDOS) between Fermi level (E_F) and $E_F + 1.5$ eV in Tersoff-Hamann approximation [21] with the constant density method [22].

Figure 1 (a) shows the monophased (4×1) reconstruction on the $\text{SrTiO}_3(110)$ surface after Ar^+ sputtering with the ion energy of 500 eV, flux of $2 \mu\text{A}$ for 10 minutes followed by UHV annealing for 1 hour [23]. The surface appears as periodic stripes along the $[1\bar{1}0]$ direction, separated with a dark trench, and each contains two obvious bright rows of periodic dots. The period is $\sim 0.6 \text{ nm}$ along $[1\bar{1}0]$ and 1.6 nm along $[001]$, respectively, corresponding to the (4×1) long-range order in respect to the bulk as observed clearly by RHEED. Evap-

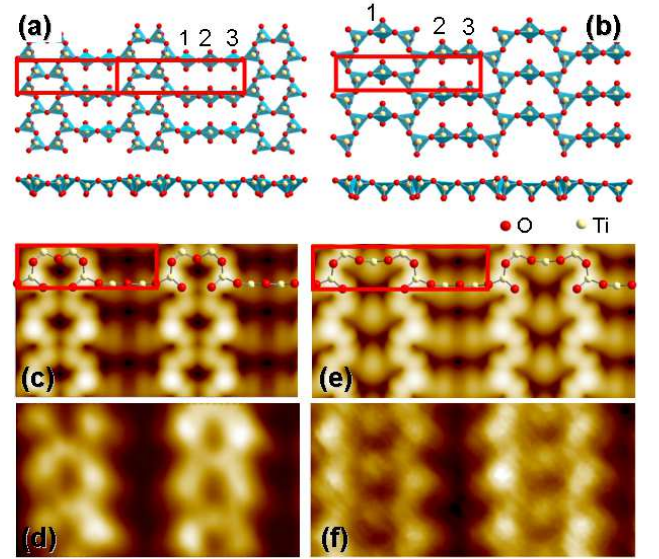


FIG. 2: (color online) (a) The structural model of the $(n \times 1)$ reconstruction [15] with (4×1) on the left and (5×1) on the right. (b) The modified structural model of (5×1) . The upper pannels are the topview while the lower pannels are the side-view. (c), (d) and (e), (f) The simulated and experimental STM images of (4×1) and (5×1) , respectively.

orating a small amount of Sr metal followed by annealing, domains with a new ordering form on the surface. As shown in Fig. 1 (b), it also appears as stripes but wider than that in the (4×1) domain, each containing three bright rows of periodic dots along the $[1\bar{1}0]$ direction. The period is $\sim 0.6 \text{ nm}$ along $[1\bar{1}0]$ and $\sim 1.95 \text{ nm}$ along $[001]$, respectively, corresponding to (5×1) reconstruction. The (5×1) domain area enlarges with the Sr evaporation dosage linearly until a monophased surface formed with $\sim 0.15 \text{ ML}$ Sr [relative to bulk-truncated $\text{SrTiO}_3(110)$, $1 \text{ ML} = 4.64 \times 10^{14} \text{ atoms/cm}^2$, see Fig. 1 (c)]. Such a phase transition can be reversed by evaporating $\sim 0.15 \text{ ML}$ Ti onto the (5×1) surface followed by annealing [17].

With DFT calculations, different structural models of (4×1) reconstruction are compared, including the Sr-adatom, TiO_x and (100) -microfaceted models. We find that the TiO_4 tetrahedra model [the left part in Fig. 2 (a)] is energetically favorable, in consistence with what Enterkin *et al.* reported previously [15]. The simulated STM images reproduce the experimental features very well, as seen in Fig. 2 (c) and (d). The unoccupied states STM image shows both titanium and oxygen atoms on the surface in bright features, as indicated by the ball-and-stick drawing superimposed onto the simulated image. The zig-zag TiO_4 chains along $[1\bar{1}0]$ correspond to the bright stripes in the STM images.

Our experimental STM images of the (5×1) reconstruction cannot be described by the $(n \times 1)$ homologous series [15] very well [the right part in Fig. 2 (a)]. We

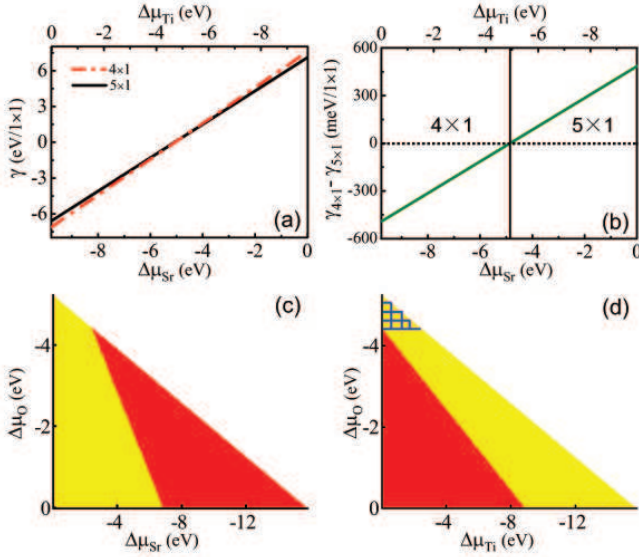


FIG. 3: (color online) (a) The surface free energy of (4×1) (red/dashed line) and (5×1) (black/solid line) as functions of $\Delta\mu_{Sr}$ and $\Delta\mu_{Ti}$, respectively ($\Delta\mu_O = -2$ eV). (b) The energy difference of (4×1) and (5×1). (c) and (d) Phase stability of (4×1) and (5×1) upon Sr & O and Ti & O environments, respectively. The black (red) zones correspond the environment in which (4×1) is stable while the grey (yellow) zones correspond to that (5×1) is stable.

modify the initial structure by shifting TiO_4 tetrahedron 1 from the linear chain along [001] to the middle of the zig-zag chain along $[1\bar{1}0]$, as shown in Fig. 2 (b). After relaxation, an extra energy gain of 0.6 eV is obtained comparing with the total energy calculated for the “(n×1)” model [15]. And the simulated STM image is in excellent agreement with the experimental one, as shown in Fig. 2 (e) and (f). It is an evidence that the monophased (5×1) surface reaches thermodynamic equilibrium rather than the mixed (n×1) phases.

In the structural models, the nominal area concentration of Ti in (4×1) is higher than that in (5×1) by 0.1 ML. Experimentally (4×1) or (5×1) phase is formed by increasing the concentration of Ti or Sr, respectively. Quantitatively the evaporation dosage to induce the phase transition (~ 0.15 ML) would be higher than the actual difference of the concentration since desorption of metal atoms occurs simultaneously. In fact the phase stability strongly depends on the metal concentration on the surface. To further clarify, we calculate the surface free energy of (4×1) and (5×1) phases under different chemical environments, respectively, in terms of chemical potential.

The surface free energy per unit area is defined by:

$$\gamma = \frac{1}{2S} [G_{slab} - N_{Ti}\mu_{Ti} - N_{Sr}\mu_{Sr} - N_O\mu_O], \quad (1)$$

where G_{slab} is the Gibbs free energy of the slab that can be calculated with our DFT calculations, N is the

number of Ti, Sr, or O atoms within the slab, μ is the chemical potential of Ti, Sr, or O, respectively, while S is the area of the symmetrical surface. For the bulk SrTiO_3 crystal, the free energy of each unit cell is:

$$G_{\text{SrTiO}_3}^{\text{bulk}} = \mu_{Sr} + \mu_{Ti} + 3\mu_O, \quad (2)$$

which equals to the energy ($E_{\text{SrTiO}_3}^{\text{bulk}}$) that can be calculated, since the surface is in the thermodynamic equilibrium with the bulk. We use relative chemical potentials $\Delta\mu_{Sr}$, $\Delta\mu_{Ti}$ and $\Delta\mu_O$, instead of the chemical potentials, with reference to the energies of a Ti atom in the hcp bulk structure, of a Sr atom in the cubic bulk structure and of an O atom in the O_2 molecule in the gas phase, respectively. And the range of accessible values for them is determined by using the method proposed by Bottin *et al.* [24].

Figure 3 (a) shows the surface free energy as a function of $\Delta\mu_{Sr}$ or $\Delta\mu_{Ti}$ with $\Delta\mu_O = -2$ eV. In a Sr-rich ($\Delta\mu_{Sr} \rightarrow 0$ eV, or Ti-poor, $\Delta\mu_{Ti} \rightarrow -9.79$ eV) environment, (5×1) is more stable than (4×1), while (4×1) is more stable in a Sr-poor (Ti-rich) environment, with the critical concentration $\Delta\mu_{Sr} = -4.86$ eV, or $\Delta\mu_{Ti} = -4.93$ eV at $\Delta\mu_O = -2$ eV. The energy difference of the two phases shown in Fig. 3 (b) is small. This explains why it has been observed experimentally that the two phases coexist with each other or even with other (n×1) phases in fragmentary domains [14].

At different oxygen partial pressure, the phase transition between (4×1) and (5×1) can be induced by the change of Sr or Ti concentration except when $\Delta\mu_O$ is extremely low, as shown in Fig. 3 (c) and (d). At our UHV condition, we always observe the (5×1) phase rather than (4×1) when $\Delta\mu_{Sr}$ is increased by evaporating Sr metal onto the surface. This is in agreement with the calculation even though the phase transition is missing in an ideal O-free environment. However, the calculation predicts that the (5×1) phase should be more stable than (4×1) when $\Delta\mu_{Ti}$ is high and $\Delta\mu_O$ is low [the labeled zone in Fig. 3 (d)], totally in contradiction to the experimental observation that increasing Ti concentration induces the formation of (4×1) phase in UHV. It is suggested that this is experimentally a “forbidden” zone – when the Ti concentration is high, the O concentration cannot be low.

It is not surprising since DFT calculations have revealed that the TiO_4 tetrahedra are energetically stable and normally appear as building blocks of the reconstruction on SrTiO_3 surfaces, *i.e.*, the surface Ti tends to be four-coordinated by oxygen on the thermodynamically stable surface. In the UHV treatment, the only possible oxygen source is the bulk SrTiO_3 . The undercoordinated surface Ti atoms will bind with oxygen atoms diffusing from bulk to form the TiO_4 tetrahedra and reduce the surface energy.

Kinetically oxygen is very diffusive in bulk SrTiO_3 [25]. A microscopic pathway has been proposed for oxygen

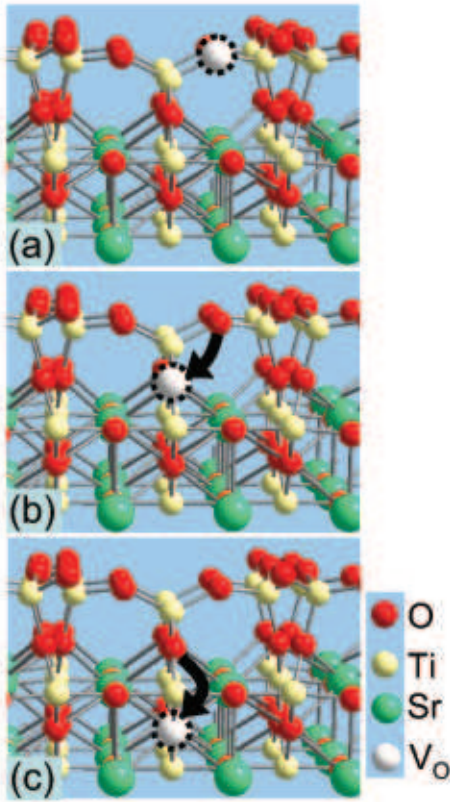


FIG. 4: (color online) A schematic diagram of the pathway of an O vacancy diffusing from SrTiO₃(110) surface towards the bulk.

vacancies between adjacent faces in a TiO₆ octahedron to form linear clusters [26]. In Fig. 4, we schematically show how an O vacancy diffuses from the (110) surface towards the bulk. Associated with two 3-coordinated Ti atoms, a surface O vacancy is unstable [Fig. 4 (a)]. It diffuses to the second layer and then to the fourth layer [Fig. 4 (b) and (c)]. The energy barrier for both processes is in the order of 0.6 eV as calculated by Cuong *et al.* [26]. Such barriers can be overcome during annealing at 1000 °C and the equilibrium is reached with O vacancies diffusing deep into the bulk. The surface undercoordinated Ti atoms actually act as pumps drawing O atoms from the bulk.

It has been a great challenge to control the density of oxygen vacancy or to minimize it to obtain an oxide surface or other LD structures with ideal stoichiometry. Highly reactive oxygen sources are employed at a high partial pressure during the growth with molecule beam epitaxy (MBE) or pulsed-laser deposition (PLD) technique. However, such a tuning is limited since the growth mode of films changes from two-dimensional layer-by-layer to three-dimensional island growth when the oxygen pressure exceeds 10⁻² mbar [27]. Moreover, specifically in MBE, the oxidation of the metal sources is also an important issue. The currently proposed “oxygen-pumping” mechanism suggests a feasible method to epi-

taxially grow high-quality titanate films along [110]. As long as the metal stoichiometry is well controlled, O vacancies can be eliminated with low growth rate at high temperature.

In conclusion, we obtain atomically well defined (4×1) and (5×1) reconstructions on SrTiO₃(110) surface. With *ab initio* calculations we resolve the microscopic structures and explain the phase transition between the two phases in terms of the surface free energy determined by metal concentration. Moreover, the surface Ti atoms draw O atoms from the bulk to form fourfold coordinations, suggesting an effective way to minimize the density of O vacancy on surfaces or in thin films of perovskite titanates.

The authors are grateful for the discussion with Jiandi Zhang (LSU). This work is supported by Chinese NSF-10704084 and Chinese MOST 2007CB936800. The calculation results are obtained on the Deepcomp7000 of Supercomputing Center, Computer Network Information Center of Chinese Academy of Sciences.

* Electronic address: jdguo@aphy.iphy.ac.cn

- [1] A. Ohtomo and H.Y. Hwang, *Nature* **427**, 423 (2004).
- [2] For a review, see *J. Phys: Condens. Matter* **20**, Issue 26, 260301-265011 (2008).
- [3] H. Habermeier, *Materials Today* **10**, 34 (2007).
- [4] A. Brinkman *et al.*, *Nature Mater.* **6**, 493 (2007).
- [5] N. Reyren *et al.*, *Science* **317**, 1196 (2007).
- [6] J. Mannhart and D.G. Schlom, *Science* **327**, 1607 (2010).
- [7] J. Heber, *Nature* **459**, 28 (2009).
- [8] W. Siemons *et al.*, *Phys. Rev. B* **76**, 155111 (2007).
- [9] M. Kawasaki *et al.*, *Science* **266**, 1540 (1994).
- [10] G. Koster *et al.*, *Appl. Phys. Lett.* **73**, 2920 (1998).
- [11] C. Noguera, *J. Phys.: Condens. Matter* **12**, R367 (2000).
- [12] J. Brunen and J. Zegenhagen, *Surf. Sci.* **389**, 349 (1997).
- [13] Y. Mukunoki *et al.*, *Appl. Phys. Lett.* **86**, 171908 (2005).
- [14] B. C. Russell and M. R. Castell, *Phys. Rev. B* **77**, 245414 (2008).
- [15] J. A. Enterkin *et al.*, *Nature Mater.* **9**, 245 (2010).
- [16] J. W. Reiner *et al.*, *Phys. Rev. Lett.* **101**, 105503 (2008).
- [17] Z. Wang *et al.*, arXiv:1012.1941 (2010).
- [18] G. Kresse and J. Furthmüller, *Phys. Rev. B* **54**, 11169 (1996); G. Kresse and J. Hafner, *Phys. Rev. B* **47**, R558 (1993).
- [19] P.E. Blöchl, *Phys. Rev. B* **50**, 17953 (1994).
- [20] J. P. Perdew *et al.*, *Phys. Rev. Lett.* **77**, 3865 (1996).
- [21] J. Tersoff and D. R. Hamann, *Phys. Rev. Lett.* **50**, 1998 (1983).
- [22] D. E. P. Vanpoucke and G. Brocks, *Phys. Rev. B* **77**, 241308(R) (2008).
- [23] Z. Wang *et al.*, *Appl. Phys. Lett.* **95**, 021912 (2009).
- [24] F. Bottin *et al.*, *Phys. Rev. B* **68**, 035418 (2003).
- [25] A. E. Paladino *et al.*, *J. Phys. Chem. Solids* **26**, 391 (1965).
- [26] D. D. Cuong *et al.*, *Phys. Rev. Lett.* **98**, 115503 (2007).
- [27] M. Huijben *et al.*, *Adv. Mater.* **21**, 1665 (2009).